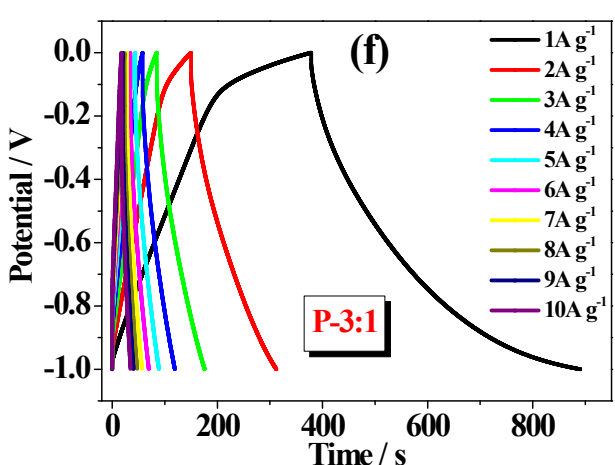
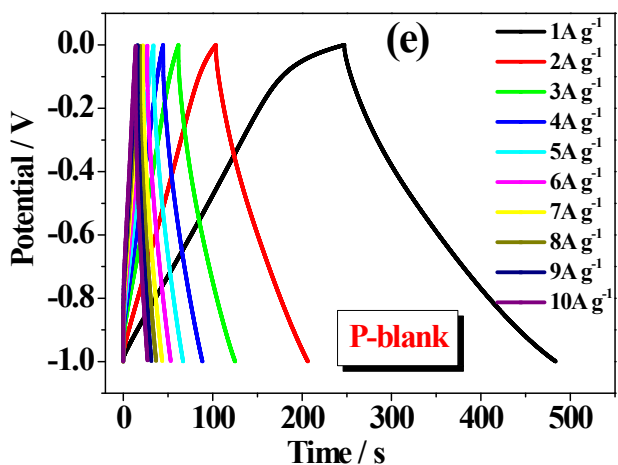
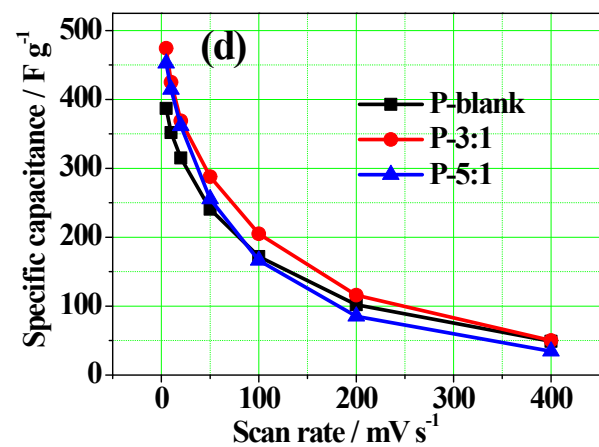
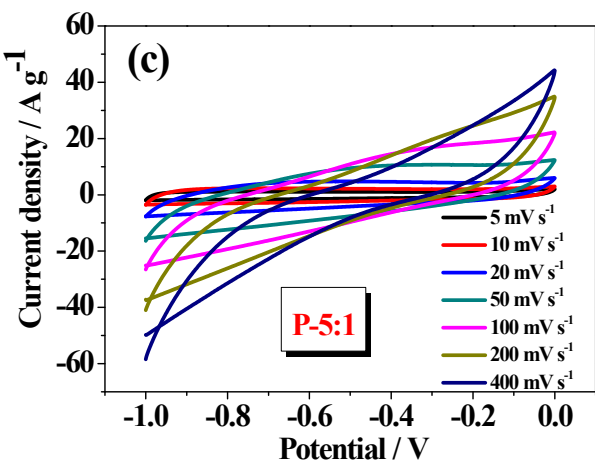
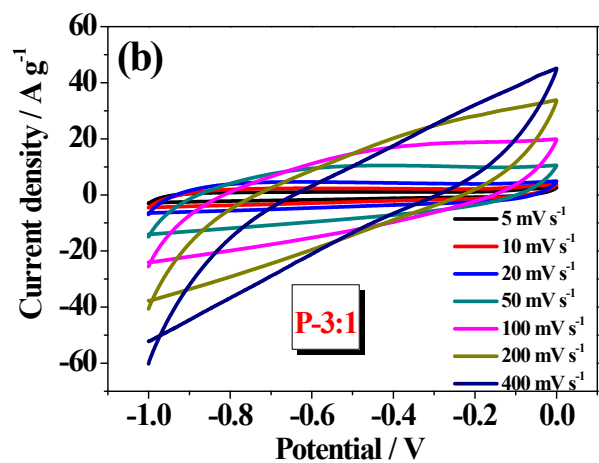
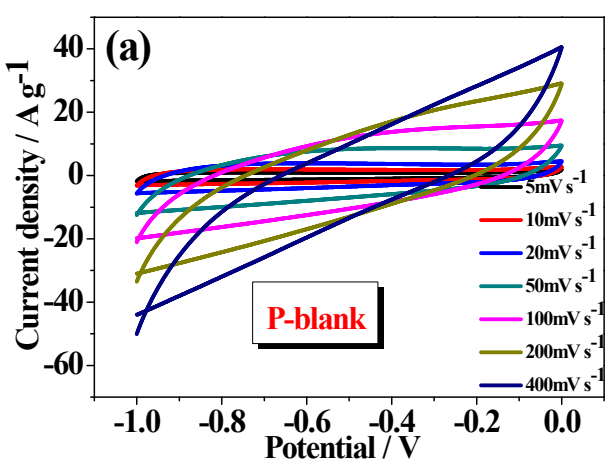


Supporting Information:

Remarkable capacitive enhancements of templated carbon materials by the redox additive electrolyte of *p*-phenylenediamine

Yong Fu Nie¹⁺, Qian Wang¹⁺, Hai Tao Yi¹, Xiang Ying Chen^{1,*},
and Zhong Jie Zhang^{2,}**



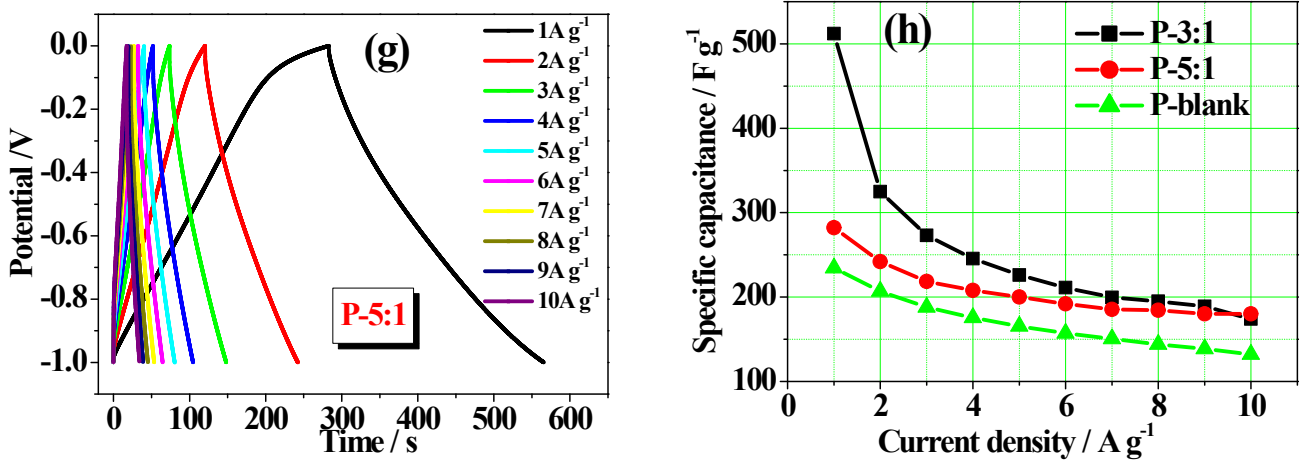


Fig. S1. P-blank, P-3:1, P-5:1 samples: (a, b, c) CV curves; (d) specific capacitances calculated from CV curves; (e, f, g) GCD curves; (h) specific capacitances calculated from GCD curves.

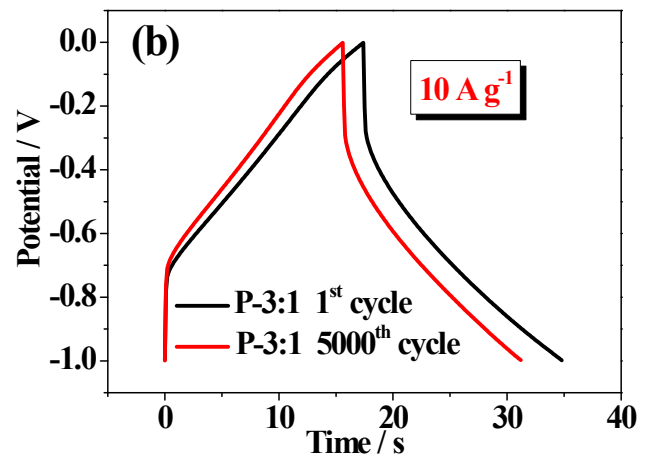
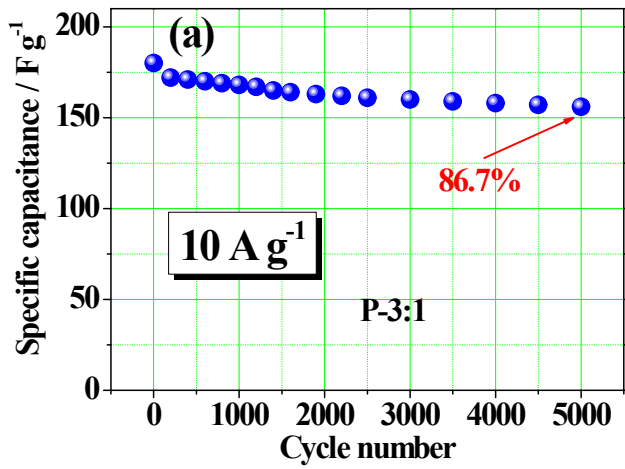


Fig. S2. P-3:1 carbon sample: (a) cycling stability measured at 10 A g^{-1} ; (b) GCD curves before/after 10^4 cycles cycling stability measured at 10 A g^{-1} .

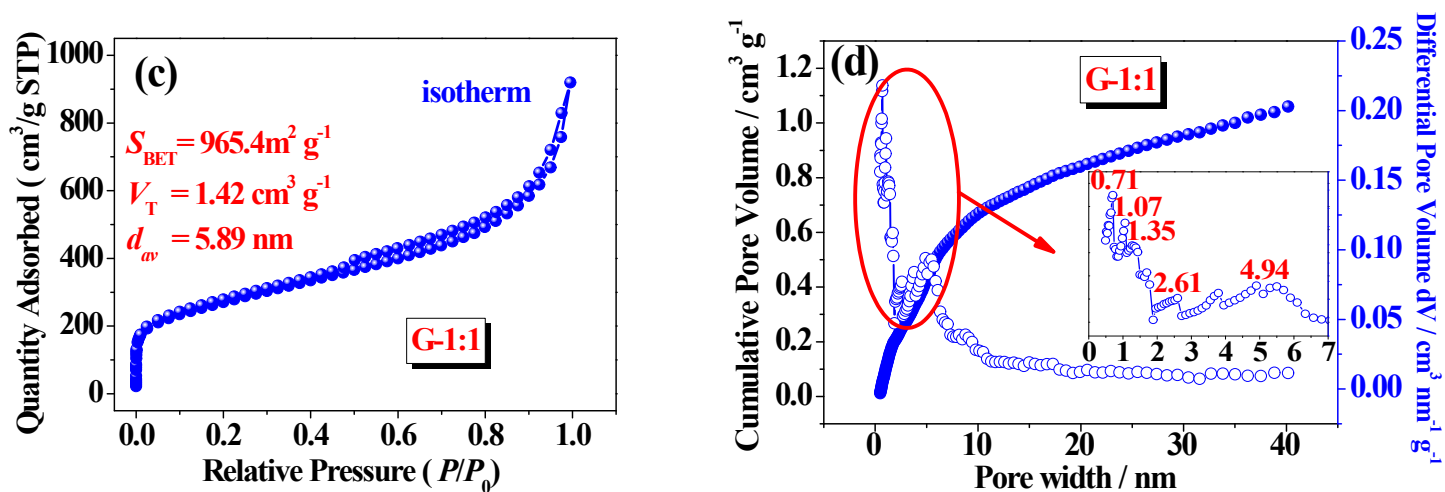
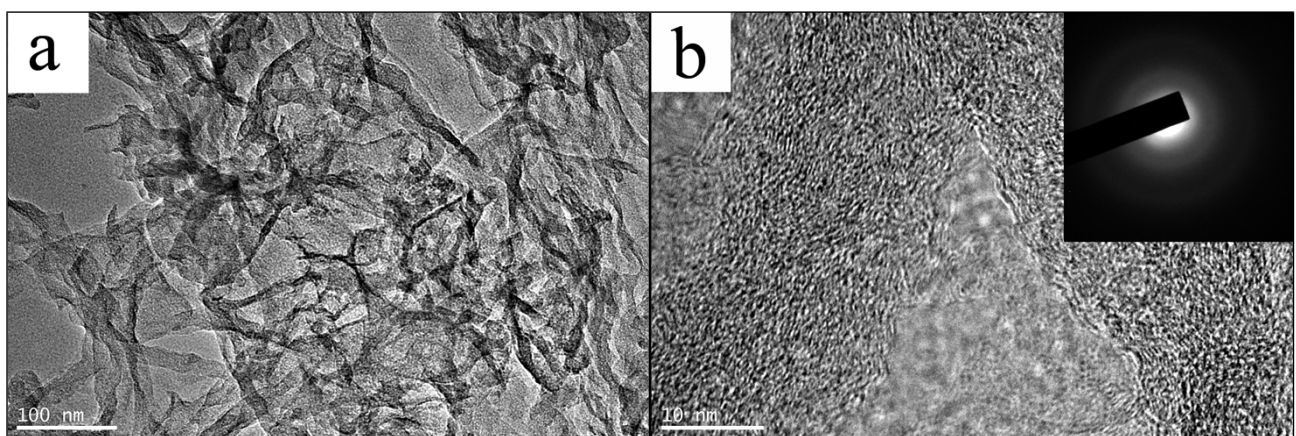


Fig. S3. The G-1:1 sample: (a-b) HRTEM images as well as the magnified SAED pattern (the insets); (c) N₂ adsorption-desorption isotherm; (d) cumulative pore volume and pore size distribution curves (estimated by using a slit/cylindrical NLDFT model).

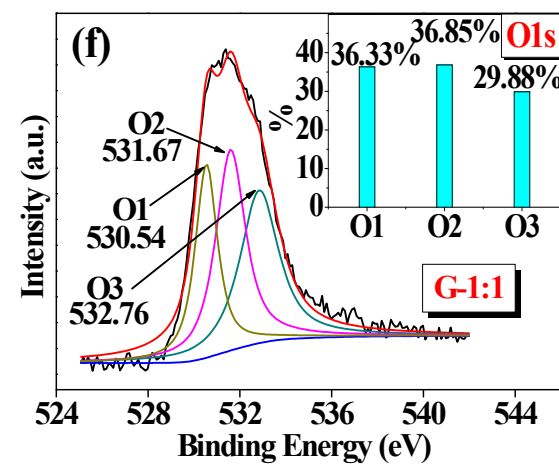
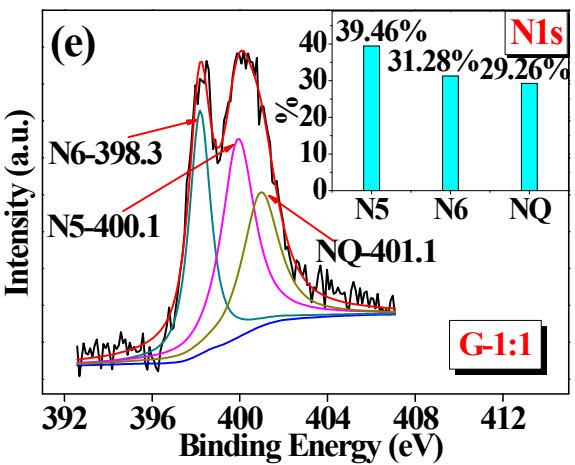
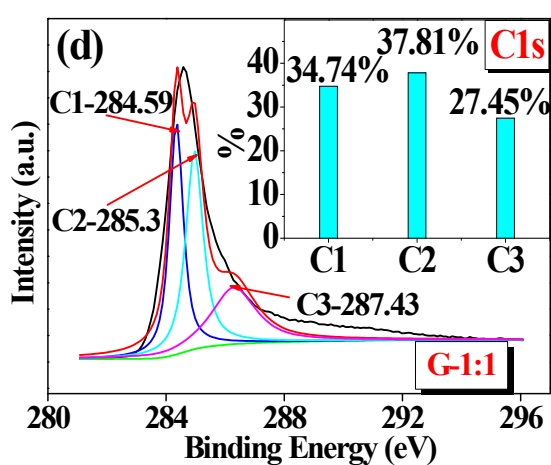
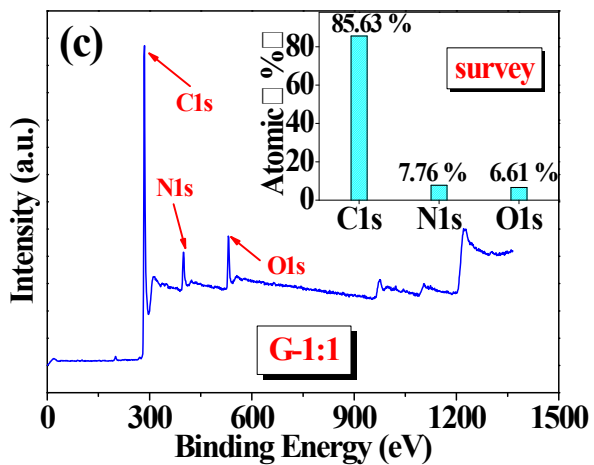
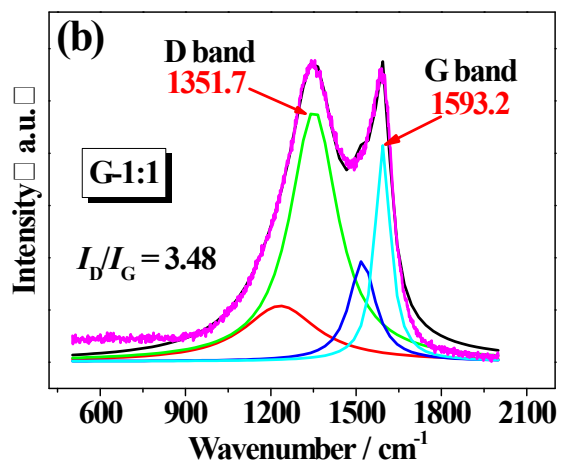
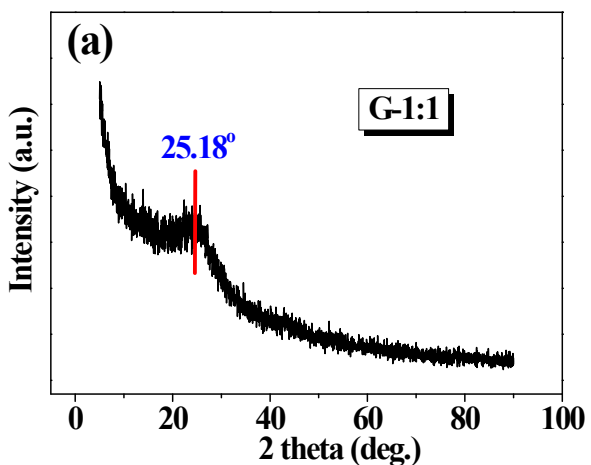
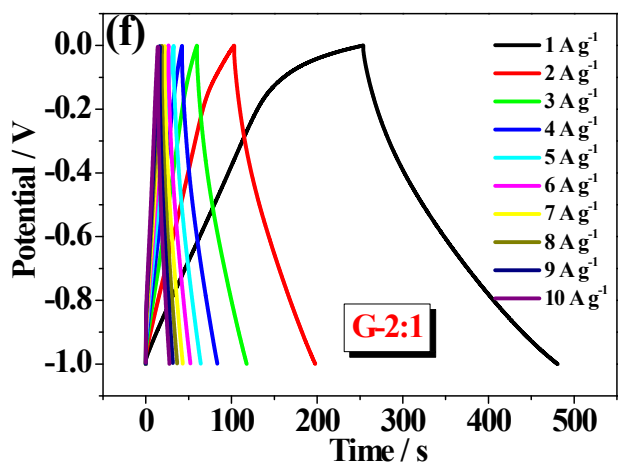
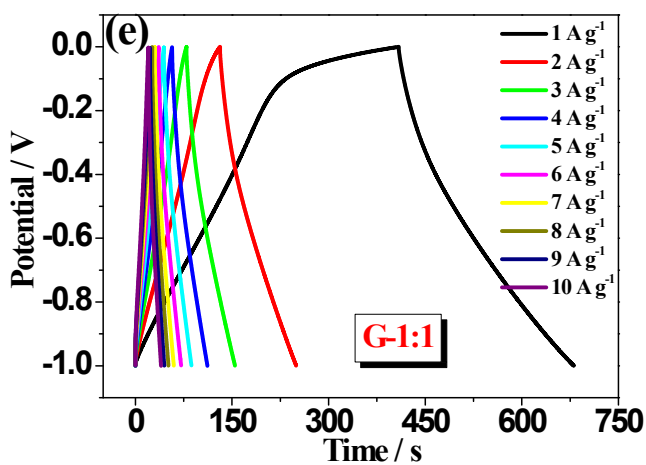
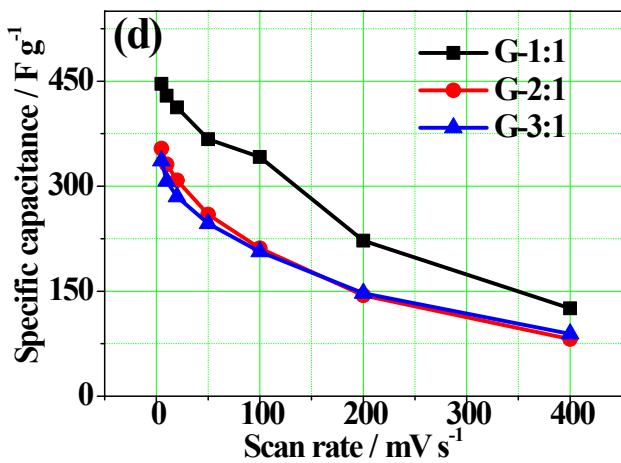
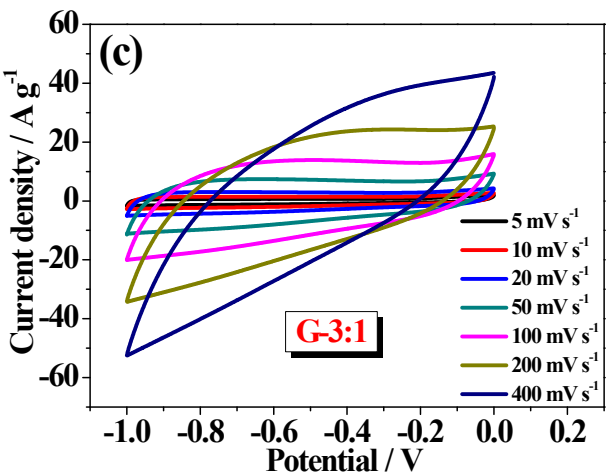
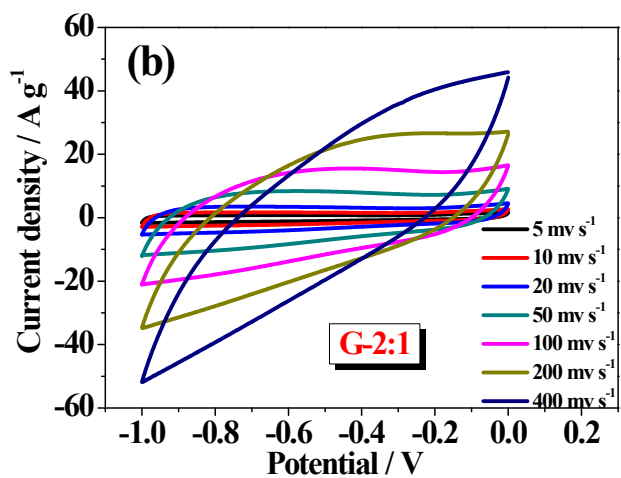
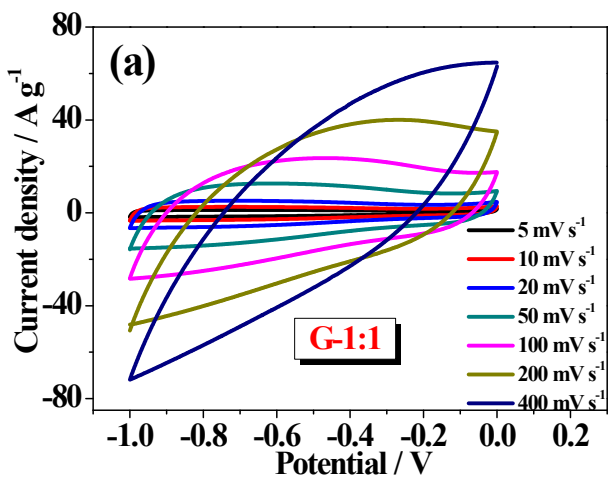


Fig. S4. The G-1:1 sample: (a) XRD pattern; (b) Raman spectrum with deconvoluted peaks; (c) survey (the insets are summary of carbon/oxygen/nitrogen contents); (d, e, f) C1s, N1s, O1s spectra with deconvoluted peaks (the insets are contents of different carbon, nitrogen, oxygen species).



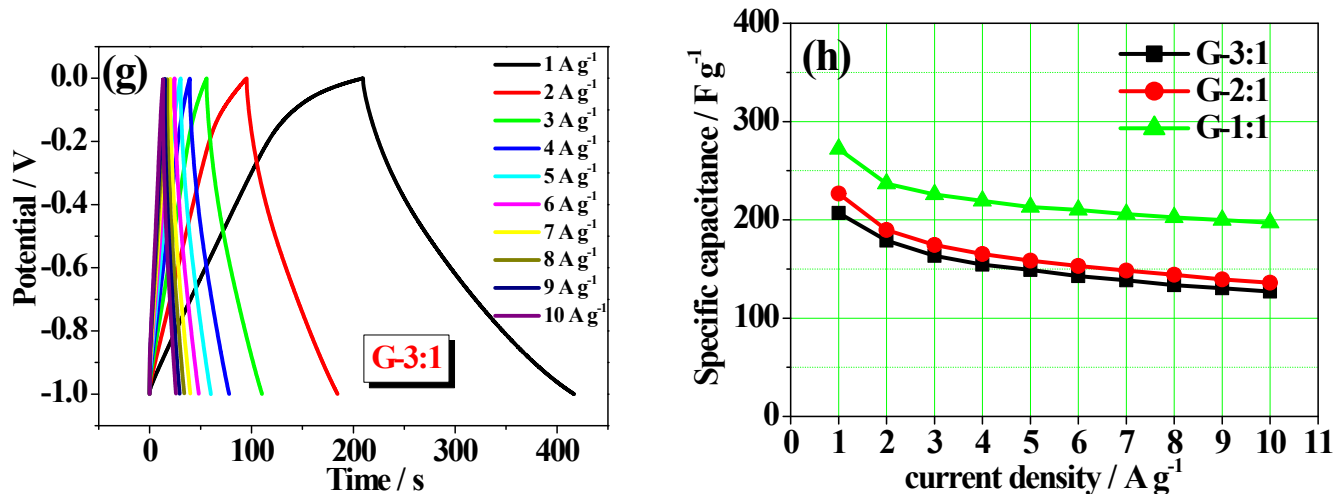


Fig. S5. G-1:1, G-2:1, G-3:1 carbon samples: (a, b, c) CV curves; (d) specific capacitances calculated from CV curves; (e, f, g) GCD curves; (h) specific capacitances calculated from GCD curves.

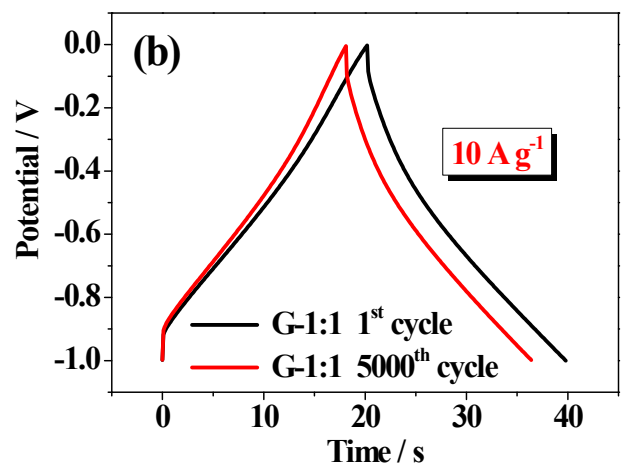
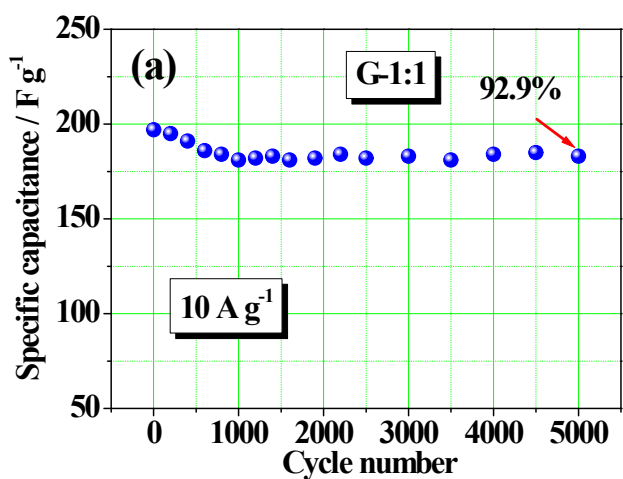


Fig. S6. G-1:1 carbon sample: (a) cycling stability measured at 10 A g^{-1} ; (b) GCD curves before/after 5000th cycles cycling stability measured at 10 A g^{-1} .

Specific energy and specific power are two significant electrochemical parameters for calculating the employment of electrochemical supercapacitors. The energy and power densities are calculated based on the following equation:

$$E = \frac{1}{2} C \Delta V^2$$

$$P = \frac{E}{\Delta t}$$

Where E (Wh kg^{-1}) is the average energy density, C (F g^{-1}) is the specific capacitance, ΔV (V) is the voltage range, P (W kg^{-1}) is the average power density, and Δt (s) is the discharge time.^{1,2}

Furthermore, the Ragone plots relating the energy density and power density are exhibited in Fig. S7a. To sum up, the **P-3:1-15** sample shows excellent Ragone results than the **P-3:1** sample. The **P-3:1-15** sample can achieve a high energy density of 118.33 Wh kg^{-1} at the power density of 1.0 kW kg^{-1} . The decrease of the energy density (90.56 Wh kg^{-1}) can be experimentally observed when increasing the power density to be 5.0 kW kg^{-1} .

Moreover, Specific energy and specific power are two significant electrochemical parameters and therefore the Ragone plots are exhibited in Fig. S7b. In a nutshell, the **G-1:1-10** sample shows superb Ragone results than the **G-1:1** sample. The **G-1:1-10** sample and the **G-1:1-10** sample can achieve a high energy density of 61.67 and 32.89 Wh kg^{-1} at the power density of 1.0 kW kg^{-1} , respectively. The decrease of the energy density can be experimentally observed when increasing the power density to be 5.0 kW kg^{-1} .

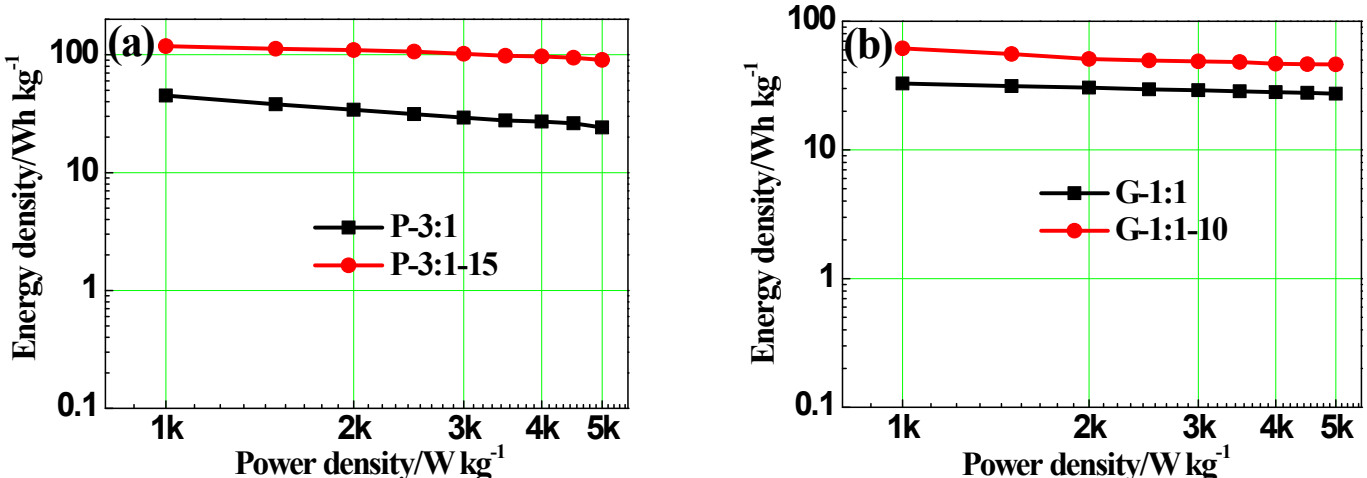


Fig. S7. Ragone plots showing energy density vs. power density: (a) The **P-3:1**, **P-3:1-15** samples; (b) The **G-1:1**, **G-1:1-10** samples.

References

- 1 Q. Wu, Y. X. Xu, Z. Y. Yao, A. R. Liu and G. H. Shi, *ACS Nano*, 2010, **4**, 1963–1970.
- 2 J. Yan, J. Liu, Z. Fan, T. Wei and L. Zhang, *Carbon*, 2010, **50**, 2179–2188.